CrossMark

ARTICLE

Well dispersed Fe_2N nanoparticles on surface of nitrogen-doped reduced graphite oxide for highly efficient electrochemical hydrogen evolution

Yi Zhang, Ying Xie, Yangtao Zhou, Xiuwen Wang, and Kai Pan[a)]
Key Laboratory of Functional Inorganic Material Chemistry, Ministry of Education, Heilongjiang University, Harbin 150080, People's Republic of China

(Received 20 January 2017; accepted 29 March 2017)

It is important to fabricate iron-based nitride/conductive material composite to obtain good catalytic performance. In this work, Fe_2N nanoparticles with diameter of approximately 30 nm have been successfully dispersed on the surface of nitrogen-doped graphite oxide (NrGO) by a facile sol–gel method and further ammonia atmosphere treatment. XPS, XRD, Raman, and TEM proved that Fe_2N nanoparticles are well monodispersed, and nitrogen atoms are doped in NrGO. The composite possessed two merits, that is, the more catalytic active site in Fe_2N nanoparticles due to the well monodispersion, and fast electron transfer due to the nitrogen dope in rGO. With the proper ratio, the composite exhibited brilliant catalytic activity and durability in acidic media. It possesses overpotential of 94 mV to approach 10 mA/cm^2, a small Tefel slope of 49 mV/dec, and maintains the good electrocatalytic activity for 10 h. Cyclic voltammetry and electrochemical impedance spectroscopy indicated that the electrocatalyst possessed high catalytic active area and fast electron transfer. Our work may provide a new avenue for the preparation of low-cost iron-based nitride/NrGO composite for highly efficient electrochemical hydrogen evolution.

I. INTRODUCTION

Hydrogen gas (H_2) fuel is a clean energy, which is a good energy source for social sustainable development.[1] Among many methods to obtain H_2 in a large scale, water splitting with applied potential is regarded as the most promising strategy.[2,3] In general, H_2 could be obtained with certain potential according the half reactions of $2H^+ + 2e^- \rightarrow H_2$ (the hydrogen evolution reaction, HER). Platinum (Pt) is most effective catalyst for water splitting, but the expensive price limits its wide application.[4–6] Thus, commercial electrocatalysts typically are inexpensive but inferior-performance materials, for example, nickel metal and its alloys.[7,8] To obtain electrocatalysts with low-cost and high catalytic efficiency, many researchers have focused on the transition metal-based materials because they possess the similar electronic structure with Pt. Among these alternatives, iron-based nitride, sulfide, and phosphide materials possess good catalytic properties and lower prices. So, they have been identified as promising materials for catalyzing the HER.[9–12] Furthermore, iron nitride is regarded as the most promised candidate because of it's facile preparation and excellent chemical stability.[13]

There also have some works about the catalytic activities of iron nitride-based materials with different structure and composition.[14–16] It is observed that the catalytic efficiency is mainly related to the chemical composition, structure, and material conductivity of catalysts. The nanostructure exhibited better catalytic performance than bulk because the more catalytic active sites had been exposed. Usually, the iron nitride materials are prepared with the pyrolysis of iron-based precursors, oxide sinteration, and chemical vapor deposition (CVD). But the Fe_2N nanocatalysts obtained with these conventional synthetic methods often possess low crystallinity and bad dispersity in size, and, the intrinsic bad conductivity limit its catalytic performance.[17,18] So, during or after their preparation, iron nitride has to be attached onto conductive supports to improve the composite conductivity and size dispersity for higher catalytic activities. For example, Fe_2N/nanocarbon composite has been prepared, and it possesses better electrocatalytic activity and chemical stability than naked Fe_2N nanomaterials.[19] Nitrogen-doped reduced graphite oxide (NrGO) is a good two dimensional conductivity material, which could result in the well dispersion of Fe_2N nanoparticles on the surface of NrGO. So, it may be a good choice to prepare Fe_2N nanoparticles/NrGO composite to improve the HER performance.

In this work, Fe_2N nanoparticles have been successfully dispersed on the surface of NrGO by a facile sol–gel

Contributing Editor: Xiaobo Chen
[a)]Address all correspondence to this author.
e-mail: kaipan@hlju.edu.cn
DOI: 10.1557/jmr.2017.138

 © Materials Research Society 2017

https://doi.org/10.1557/jmr.2017.138 Published online by Cambridge University Press

method and further NH_3 treatment. In this route, $Fe(OH)_3$ sol/graphite oxide (GO) was first prepared, which granted the perfect dispersion of $Fe(OH)_3$ on the GO surface. Then, during the following heat treatment, the precursor mixtures could be easily converted into the desired monodispersed iron nitride nanoparticles without nanoparticle aggregation. Furthermore, GO could be spontaneously be converted into NrGO, which possessed better conductivity for fast electron transfer. In result, the Fe_2N/NrGO composite possessed two merits, that is, the more catalytic active site in Fe_2N nanoparticles, and fast electron transfer in NrGO. The ratio of Fe_2N and NrGO could be controlled by the amount of iron source and GO. With the modest ratio, the composite exhibited brilliant catalytic activity and durability in acidic media. It possesses the overpotential of 94 mV to obtain the current density of 10 mA/cm^2, and its activity could be maintained for at least 10 h. That results could be compared with many other nitride catalysts in recently reports. This work may pave a new road for the preparation of monodispersed cheap iron-based nitride/NrGO composite for highly efficient HER.

II. EXPERIMENTAL SECTION

A. Chemicals

The ethanol, ammonia, $FeCl_3$, and H_2SO_4 were bought from Tianjin Kermel Chemical Reagent Company (Tianjin, China), *N*-methyl-2-pyrrolidone and polyvinylidene fluoride were purchased from Aladdin Company (Shanghai, China), and the carbon paper was purchased from Shanghai Hesen Company (Shanghai, China).

B. The preparation of Fe_2N/NrGO

Graphite oxide (GO) and $Fe(OH)_3$ sol were firstly prepared, respectively. GO was prepared by a modified Hummers method.[20] For the preparation of $Fe(OH)_3$ sol, 2 M of $FeCl_3$ solution was dropped into 400 mL of boiling distilled water. Then, the $Fe(OH)_3$ sol was prepared after the solution was kept boiling for 5 min. For the synthesis of Fe_2N/NrGO, 1 g of GO was firstly dispersed in 500 mL of distilled water by sonication. Then 1 mL of $Fe(OH)_3$ sol and 5 mL of 37% ammonia were dropped into above solution, followed by stirring for 90 min. A solid was obtained after the solution was dried in an oven overnight. At last, Fe_2N/NrGO composite was prepared after the solid was calcined at 800 °C for 3 h under NH_3 atmosphere. The obtained sample is labeled Fe_2N/NrGO. For the investigation of the best HER catalytic performance of Fe_2N/NrGO composite, Fe_2N/NrGO composite with different Fe_2N content were also obtained by adding different amount of precursor Fe $(OH)_3$ sol of 0.5 mol or 1.5 mol to precursor GO solution of 1 g. The obtained samples are named Fe_2N/NrGO* and Fe_2N/NrGO**, respectively.

C. Physical characterizations

A Bruker D8 diffractometer (Bruker corporation, Karlsruhe, Germany) using Cu K_α (λ = 1.5406 Å) radiation was used to measure the X-ray diffraction (XRD) patterns of samples. A Jobin Yvon HR 800 micro-Raman spectrometer (Horiba Jobin Yvon, Paris, France) at 457.9 nm was used to measure the Raman spectra. A VG ESCALAB MK II (VG Instruments, London, United Kingdom) with an Mg K_α (1253.6 eV) achromatic X-ray source was performed to analyze the X-ray photoelectron spectroscopy (XPS). Scanning electron microscopy (SEM) with an acceleration voltage of 5 kV and transmission electron microscopy (TEM) with an acceleration voltage of 200 kV were used to character the morphology and structure of samples.

D. Electrochemical measurements

An electrochemical station (BAS100B, CH Instruments, Shanghai, China) was used for the electrochemical measurements in a three-electrode system with a saturated calomel electrode (SCE) as the reference electrode, a carbon rod electrode as the counter electrode, and carbon paper coated with Fe_2N/NrGO catalyst as the working electrode. The Fe_2N/NrGO electrode was fabricated as follows: Fe_2N/NrGO was firstly dispersed in *N*-methyl-2-pyrrolidone solvent with 5 wt% polyvinylidene fluoride under sonication and stirring to get a slurry, in which the weight ratio of Fe_2N/NrGO to polyvinylidene fluoride was 8:1. Then the slurry was coated onto the surface of a carbon paper. The effective loading area was about 1 cm^{-2} and the loading density of Fe_2N/NrGO nanocatalyst was 3 mg/cm^2, which is calculated by weighing the difference of the carbon paper before and after coating. Linear sweep voltammetry was carried out in 0.5 M H_2SO_4 solution (deaerated by N_2 gas) with a scanning rate of 5 mV/s. Based on the electrochemical impedance spectra, all the data have been corrected for a small ohmic drop. All the potentials have been calibrated to a reversible hydrogen electrode (RHE).

III. RESULTS AND DISCUSSION

The synthesis process included the preparation of $Fe(OH)_3$ sol/GO and the following reaction with ammonia to obtain Fe_2N/NrGO composite. In this two-step process, Fe_2N/NrGO composite with different Fe_2N weight contents have been obtained by controlling the addition amount of $Fe(OH)_3$ colloids into GO, and then the composites are calcined at 800 °C under ammonia atmosphere. XPS measurements can accurately test the element valence state so it is used to further explore the composition of products. As shown in Figs. 1(a) and 1(c), Fe, O, and N elements exist in the obtained composite. It can be found in Fig. 1(b) that there are two binding energy peaks at 710.5 eV and 724.1 eV, which

https://doi.org/10.1557/jmr.2017.138 Published online by Cambridge University Press

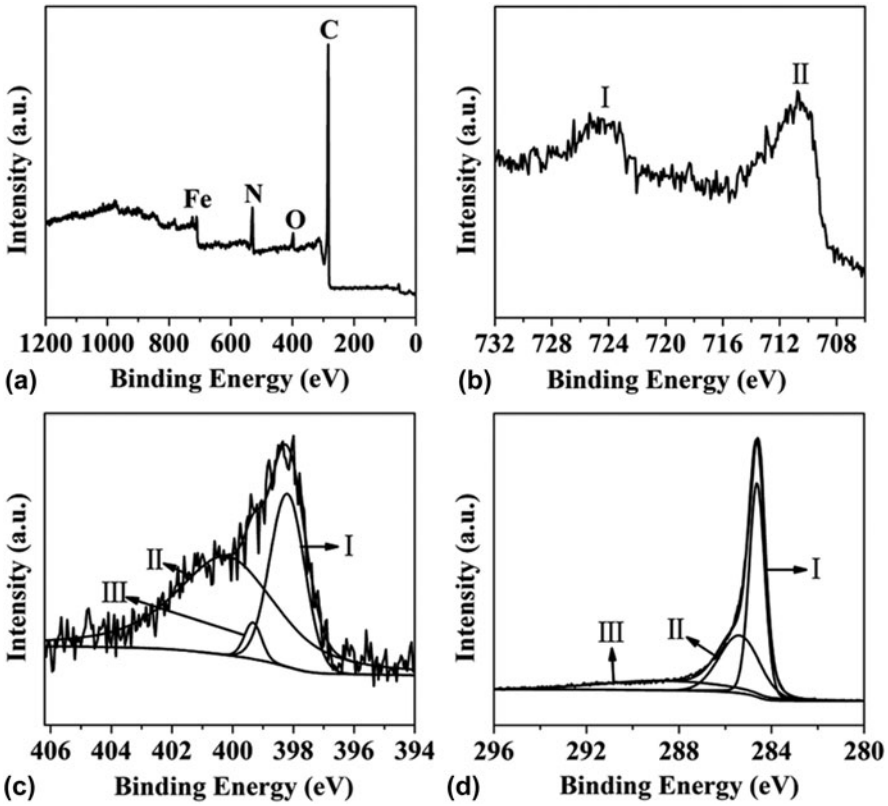


FIG. 1. XPS of Fe_2N/NrGO (a) wide scan, (b) Fe 2*p*, (c) N 1*s*, and (d) C 1*s*.

corresponded to the Fe $2p_{3/2}$ and $2p_{1/2}$ level, respectively. The N 1*s* binding energy spectrum is displayed in Fig. 1(c), which could be fitted into three peaks. Peak I at 398.2 eV is attributed to metal nitride, which existed in Fe_2N. Moreover, peak II at 399.3 eV and peak III at 400.0 eV can be ascribed to pyridinic-N and pyrrolic-N, respectively, which existed in NrGO. The XPS results indicate that the N atoms combine with C atoms in NrGO.[21–24] The high-resolution C 1*s* XPS spectra is shown in Fig. 1(d). Binding energy peak I at 284.6 eV is ascribed to C–C bonding energy for the defect-free graphite, Peak II at 285.4 eV is ascribed to carbon bonding energy of C–N bonds. Peaks III at 288.6 eV should be attributed to the carbon binding energy of C=O bonds. The C binding energy spectra further confirm the combination of N atoms with C atoms in NrGO. The XPS data proved that Fe_2N/NrGO composite had been prepared.

XRD and Raman spectra are used to characterize the composite composition. The XRD patterns of Fe_2N/NrGO, Fe_2N, and NrGO are exhibited in Fig. 2. For the composite, the peaks at $2\theta = 38.5$, 40.71, 43.18, 56.17, 68.2, and 75.8° are indexed to the (110), (002), (110), (112), (300), and (113) planes of Fe_2N [(JCPDS) no.89-3939], respectively. The diffraction peak at $2\theta = 26.4°$ is ascribed to the graphite (002) plane.[25] Fig. 3 shows the Raman spectra of Fe_2N/NrGO, Fe_2N, and NrGO, respectively. Below 1000 cm^{-1}, the peaks of Fe_2N/NrGO perfectly match the peak of pure Fe_2N. The wavelengths

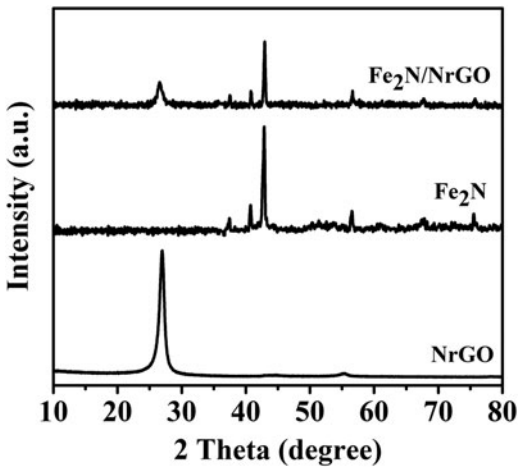


FIG. 2. The XRD patterns of NrGO, Fe_2N/NrGO, and Fe_2N.

at 1310 cm^{-1} and 1595 cm^{-1} indicated the disordered D and G band of carbon that proved the formation of Fe_2N/NrGO composite at the same time.[26] So, Fe_2N/NrGO composite is obtained by the facile sol–gel method.

The microstructure of Fe_2N/NrGO can be observed from TEM images. It can be seen in Fig. 4(a) that the monodispersed Fe_2N nanoparticles with size of about 30 nm were embedded on the surface of NrGO. When Fe_2N/NrGO composites are obtained, the graphite oxide

https://doi.org/10.1557/jmr.2017.138 Published online by Cambridge University Press

layers remain flat, and all the Fe_2N nanoparticles grew on the surface of NrGO, no separated Fe_2N nanoparticles without NrGO could be found. From the high-resolution TEM (HRTEM) image [Fig. 4(b)], we can observe the plane distances of 0.24 nm and 0.34 nm, which corresponded to the (002) crystal facet of Fe_2N and (002) crystal facet of NrGO, respectively.[27] Iron nitride is a kind of good catalyst, but monodispersed iron nitride nanoparticles could be aggregated easily during the high temperature synthesis process. To solve this problem, we use NrGO as conductive substrate, which makes the iron nitride nanoparticles distribute uniformly on the surface of NrGO. This could get the low resistance for the electron transfer during the HER process. So we think this kind of small size, uniformly-distributed iron nitride nanoparticles/NrGO possessed a great advantage for HER.

To obtain the best catalytic performance of Fe_2N/NrGO composite for the HER measurement, composite with different Fe_2N and NrGO ratio has been prepared. Figure 5 shows the polarization and Tafel curve of Fe_2N/NrGO with different ratio. It can be seen that when we add 1 mol $Fe(OH)_3$ sol to 1 g GO, the obtained catalytic sample (named Fe_2N/NrGO) displayed the best catalytic performance than any other samples (Fe_2N/NrGO* and Fe_2N/NrGO**). Its overpotential is minimal and the current density is the largest. Also, the catalytic performance of Fe_2N/NrGO is far better than that of single Fe_2N or NrGO alone. So, the best composite sample Fe_2N/NrGO is used for the below measurement. As a conventional HER catalyst, Pt sheet has excellent catalytic performance whose overpotential tends to zero

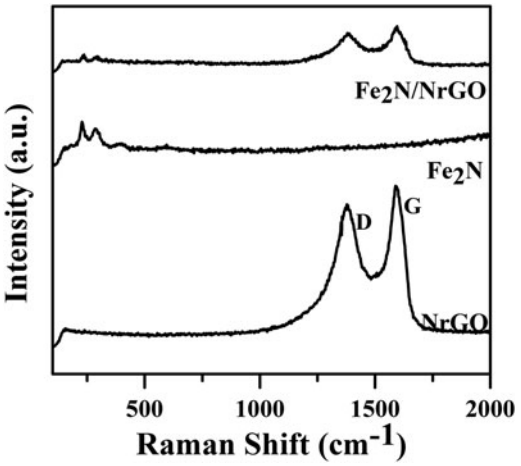


FIG. 3. The Raman shifts of NrGO, Fe_2N/NrGO, and Fe_2N.

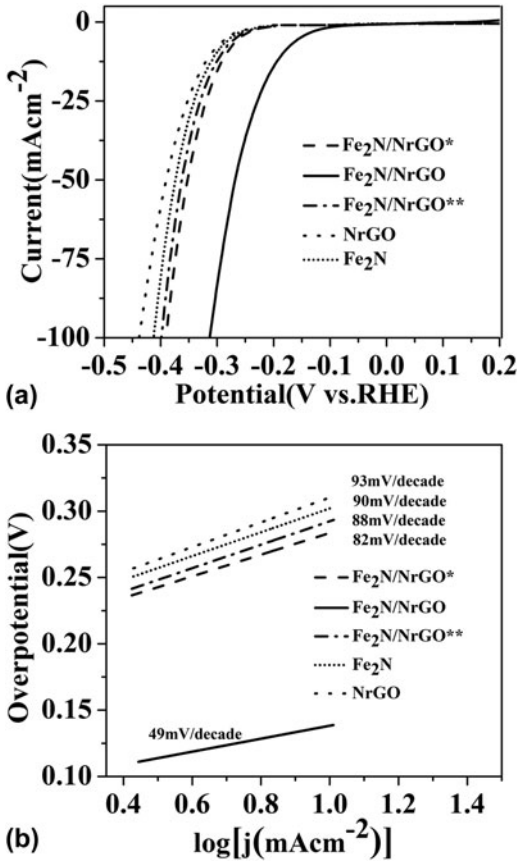


FIG. 5. (a) Polarization curves for different proportion of Fe_2N and NrGO with a scan rate of 5 mV/s. (b) Tafel plots for different proportion of Fe_2N and NrGO with a scan rate of 1 mV/s.

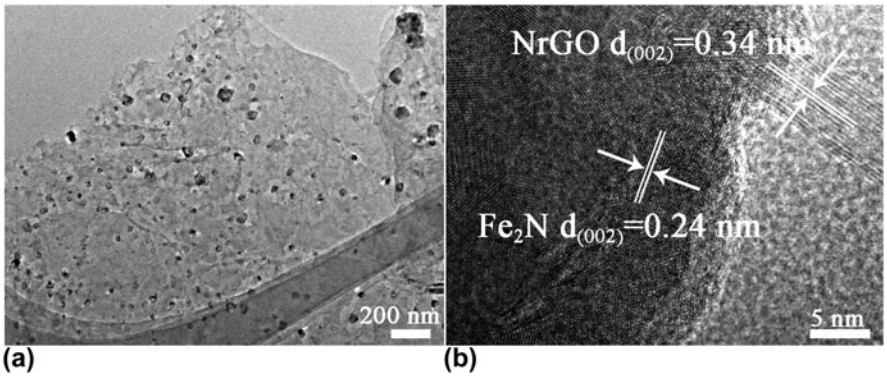


FIG. 4. (a) TEM images of Fe_2N/NrGO and (b) the HRTEM image of Fe_2N/NrGO.

https://doi.org/10.1557/jmr.2017.138 Published online by Cambridge University Press

[Fig. 6(a), green curves]. As a HER inert material, carbon paper shows very weak catalytic performance, but it has good conductivity, it is a good substrate for HER [Fig. 6(a), black curves]. The Fe_2N/NrGO composite structure has an effective catalytic performance with an overpotential of 94 mV to reach the current density of 10 mA/cm^2 [Fig. 6 (a)], which is also smaller than the data for hierarchical nanostructure iron based sample $FeNi_3N$/Ni foam (202 mV),[14] Ni_3FeN nanoparticles (158 mV)[15] and binary nickel–iron nitride nanoarrays (180 mV)[16] reported in the previous literature. The details of HER mainly include protons combination with Fe_2N, generation of hydrogen atoms in the surface of Fe_2N, and hydrogen release. Because nitrogen-doped rGO has many functional groups that are easier to combine with iron ionics, $Fe(OH)_3$ could be monodispersed on the surface of NrGO, which exposed more catalytic active sites for improved HER efficiency. The monodispersed Fe_2N nanoparticles could fully contact with the protons of electrolyte, NrGO conductive substrate could improve the electron transfer, which are advantageous for the reaction between the protons and Fe_2N catalysts to bring down HER overpotential, to reduce the Tafel, and to improve the reaction efficiency.[28] For further study of the HER activity of the Fe_2N/NrGO electrocatalyst, Tafel plots are fitted to the equation $\eta = b\log(j) + a$, where b is the Tafel slope and j is the current density. Figure 6(b) indicates that the Tafel slope of Pt is about 30 mV/dec, which is in accordance with the literature values. The Tafel slope of Fe_2N/NrGO is around 51 mV/dec, which is smaller than that of hierarchical nanostructure iron based sample $FeNi_3N$/Ni foam (98 mV/dec),[14] and binary nickel–iron nitride nanoarrays (101 mV/dec).[16] The HER dynamic process belongs to Volmer–Heyrovsky mechanism, and the rate-limiting step of hydrogen is electrochemical desorption.[29–31]

HER electrochemical stability is also an indispensable standard to evaluate the catalyst properties. The HER electrochemical stability of Fe_2N/NrGO nanocomposite is tested using chronopotentiometry [Figs. 6(c) and 6(d)]. The current density of Fe_2N/NrGO only slightly decreased a little after 10 h, which indicated that Fe_2N/NrGO composite possesses excellent electrochemical stability [Fig. 6(c)]. Furthermore, the catalytic times of Fe_2N/NrGO was carried out at a fixed potential of 120 mV. It could be seen that the current density at 10 mA/cm^2 remained relatively stable for 10 h [Fig. 6(d)]. So, the good durability of Fe_2N/NrGO catalyst shows promise for practical applications over a long period.

Generally, the exchange current density of catalysts is proportional to the catalytic active area. The catalytic active area is conventionally estimated by measuring the capacitance of the double layer at the solid–liquid interface via a simple cyclic voltammetry (CV) method. The current density was responded under the potential range of 0.2–0.3 V (versus RHE) with different scanning rates from 20 to 120 mV [Fig. 7(a)]. Then, the curves are

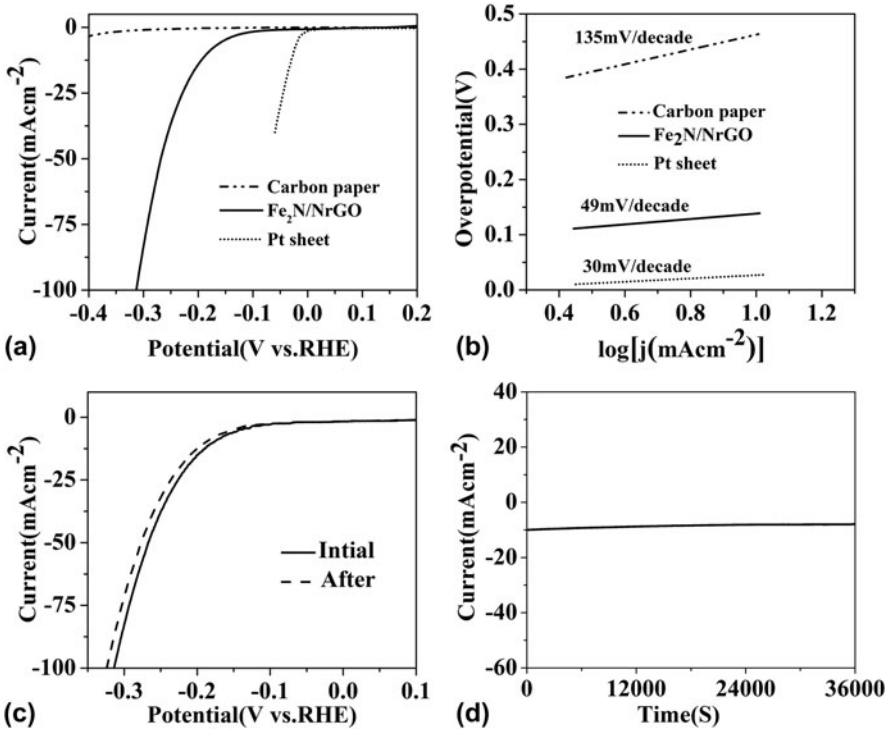


FIG. 6. (a) Polarization curves for Fe_2N/NrGO, carbon paper, and Pt in 0.5 M H_2SO_4 with a scan rate of 5 mV/s. (b) Tafel plots for Fe_2N/NrGO, carbon paper, and Pt with a scan rate of 1 mV/s. (c) The polarization curves of Fe_2N/NrGO before and after 10 h in 0.5 M H_2SO_4 solution. (d) Cycling stability of Fe_2N/NrGO at an overpotential of 120 mV.

https://doi.org/10.1557/jmr.2017.138 Published online by Cambridge University Press

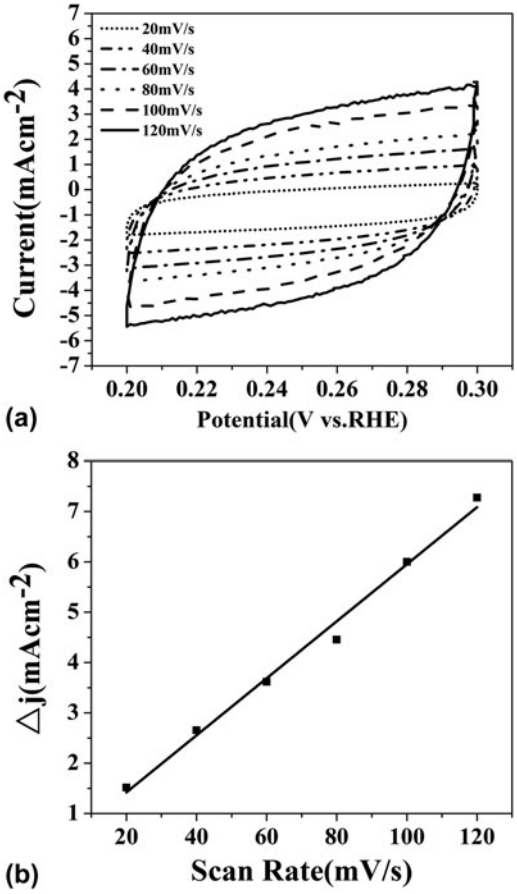


FIG. 7. (a) CVs for Fe_2N/NrGO with different rates from 20 to 120 mV/s^2. (b) The capacitive current at 0.25 V as a function of scan rate for Fe_2N/NrGO ($\Delta j_0 = j_a - j_c$).

obtained by plotting the $\Delta j = j_a - j_c$ at a given potential (0.25 V versus RHE) against the CV scanning rates [Fig. 7(b)]. The capacitance of Fe_2N/NrGO electrode is 56.6 mF/cm^2, which means that Fe_2N/NrGO electrode possessed relatively high catalytic active area.[32] It is because the obtained nanocomposite possessed two merits, the more catalytic activity sites of Fe_2N and fast electron transfer of NrGO.

Electrochemical impedance spectroscopy (EIS) was further carried out at HER overpotential of 360 mV to illustrate the relative enhanced electron transfer. The Nyquist plots of Fe_2N/NrGO, carbon paper substrate and Pt electrode are shown in Fig. 8. Experimental data were fitted with the equivalent circuit of R_s (R_{ct}CPE), where R_s represents the ohmic resistance, R_{ct} reflects the charge transfer resistance between Fe_2N/NrGO and the electrolyte interface, CPE is a constant phase element.[33,34] Generally, a smaller R_{ct} means a faster charge transfer. The Fe_2N/NrGO electrode displays a smaller R_{ct} than that of Fe_2N, NrGO and carbon paper, only a little inferior than that of Pt. It indicated that Fe_2N/NrGO electrode could provide a faster electron transfer than that

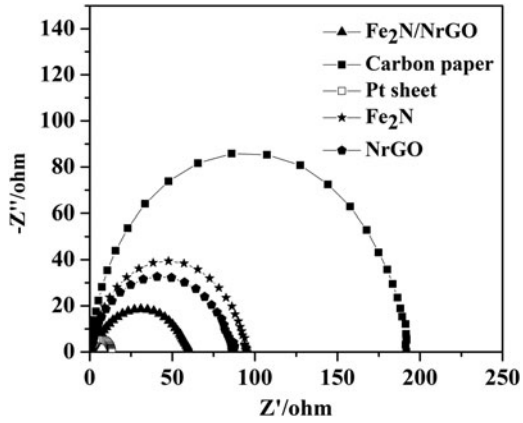


FIG. 8. Electrochemical impedance spectra (EIS) of Fe_2N, NrGO, Fe_2N/NrGO, carbon paper, and Pt catalyzed HER at overpotential of 360 mV.

of carbon paper, which is due to the combination of Fe_2N and NrGO that makes the electron transfer faster.

IV. CONCLUSION

In this work, a facile and efficient method has been developed to synthesize monodispersed Fe_2N nanoparticles/NrGO composite as a cheap and highly efficient catalyst for the hydrogen evolution reaction (HER). With the controlled ratio, monodispersed Fe_2N/NrGO composite has high HER catalytic activity and great stability with a small onset overpotential of 94 mV to reach current density of 10 mA/cm^2, and its Tafel slope is 51 mV/dec. It could be attributed to the specific composite structure that possessed two merits: more catalytic active sites of Fe_2N nanoparticles and fast electron transfer of NrGO. Moreover, this kind of synthetic route could be extended to synthesis iron carbide and iron sulfide for greater performance catalyst for HER.

ACKNOWLEDGMENTS

We gratefully acknowledge the support of this research by the National Natural Science Foundation of China (21473051) and the Excellent Youth of Common Universities of Heilongjiang Province (1252G045).

REFERENCES

1. C.G. Morales-Guio, L.A. Stern, and X. Hu: Cheminform abstract: Nanostructured hydrotreating catalysts for electrochemical hydrogen evolution. *Chem. Soc. Rev.* **43**, 6555 (2014).
2. M. Zeng and Y.G. Li: Recent advances in heterogeneous electrocatalysts for hydrogen evolution reaction. *J. Porphyrins Phthalocyanines* **3**, 510 (2015).
3. M.A. Lukowski, A.S. Daniel, C.R. English, F. Meng, A. Forticaux, R.J. Hamers, and S. Jin: Highly active hydrogen evolution catalysis from metallic WS_2 nanosheets. *Energy Environ. Sci.* **7**, 2608 (2014).

https://doi.org/10.1557/jmr.2017.138 Published online by Cambridge University Press

4. X.X. Zou, X.X. Huang, A. Goswami, R. Silva, B.R. Sathe, E. Mikmeková, and T. Asefa: Cobalt-embedded nitrogen-rich carbon nanotubes efficiently catalyze hydrogen evolution reaction at all pH values. *Angew. Chem., Int. Ed.* **126**, 4372 (2014).
5. J. Duan, S. Chen, M. Jaroniec, and S.Z. Qiao: Porous C_3N_4 nanolayers@N-graphene films as catalyst electrodes for highly efficient hydrogen evolution. *ACS Nano* **9**, 931 (2015).
6. W. Zhou, J. Zhou, Y. Zhou, J. Lu, K. Zhou, L.J. Yang, Z.H. Tang, L.G. Li, and S.W. Chen: N-doped carbon-wrapped cobalt nanoparticles on N-doped graphene nanosheets for high-efficiency hydrogen production. *Chem. Mater.* **27**, 2026 (2015).
7. X. Fan, Z. Peng, R. Ye, H. Zhou, and X. Guo: M_3C (M: Fe, Co, Ni) nanocrystals encased in graphene nanoribbons: An active and stable bifunctional electrocatalyst for oxygen reduction and hydrogen evolution reactions. *ACS Nano* **9**, 7407 (2015).
8. J. Deng, P. Ren, D. Deng, L. Yu, F. Yang, and X.H. Bao: Highly active and durable non-precious-metal catalysts encapsulated in carbon nanotubes for hydrogen evolution reaction. *Energy Environ. Sci.* **7**, 1919 (2014).
9. M.S. Faber, M.A. Lukowski, D. Qi, N.S. Kaiser, and J. Song: Earth-abundant metal pyrites (FeS_2, CoS_2, NiS_2, and their alloys) for highly efficient hydrogen evolution and polysulfide reduction electrocatalysis. *J. Phys. Chem. C* **118**, 21347 (2014).
10. R. Liu, S. Gu, H. Du, and C. Li: Controlled synthesis of FeP nanorod arrays as highly efficient hydrogen evolution cathode. *J. Mater. Chem. A* **2**, 17263 (2014).
11. X. Yang, A.Y. Lu, Y. Zhu, S. Min, M.N. Hedhili, Y. Han, K.W. Huang, and L.J. Li: Rugae-like FeP nanocrystal assembly on a carbon cloth: An exceptionally efficient and stable cathode for hydrogen evolution. *Nanoscale* **7**, 10974 (2015).
12. C. Lv, Z. Peng, Y.X. Zhao, Z.P. Huang, and C. Zhang: The hierarchical nanowires array of iron phosphide integrated on a carbon fiber paper as an effective electrocatalyst for hydrogen generation. *J. Mater. Chem. A* **4**, 1454 (2015).
13. P. Yu, L. Wang, F. Sun, D. Zhao, C.G. Tian, L. Zhao, X. Liu, J.Q. Wang, and H.G. Fu: Three dimensional Fe_2N@C microspheres grown on reduced graphite oxide for lithium ion batteries and the Li storage mechanism. *Chem. –Eur. J.* **21**, 3249 (2015).
14. B. Zhang, C. Xiao, S. Xie, J. Liang, X. Chen, and Y.H. Tang: Iron–nickel nitride nanostructures in situ grown on surface-redox-etching nickel foam: Efficient and ultrasustainable electrocatalysts for overall water splitting. *Chem. Mater.* **28**, 6934 (2016).
15. X. Jia, Y. Zhao, G. Chen, L. Shang, R. Shi, X. Kang, G.I.N. Waterhouse, L.Z. Wu, C.H. Tung, and T.R. Zhang: Ni_3FeN nanoparticles derived from ultrathin NiFe-layered double hydroxide nanosheets: An efficient overall water splitting electrocatalyst. *Adv. Energy Mater.* **6**, 1502585 (2016).
16. M. Jiang, Y.J. Li, Z.Y. Lu, X.M. Sun, and X. Duan: Binary nickel–iron nitride nanoarrays as bifunctional electrocatalysts for overall water splitting. *Inorg. Chem. Front.* **3**, 630 (2016).
17. L. Wang, J. Yin, L. Zhao, C. Tian, P. Yu, J. Wang, and H. Fu: Ion-exchanged route synthesis of Fe_2N-N-doped graphitic nanocarbons composite as advanced oxygen reduction electrocatalyst. *Chem. Commun.* **49**, 3022 (2013).
18. M. Agemi, K. Kayama, M. Noborisaka, Y. Tachimoto, A. Shirakura, and T. Suzuki: Synthesis of hydrogenated amorphous carbon films with a line type atmospheric-pressure plasma CVD apparatus. *Surf. Coat. Technol.* **206**, 2025 (2011).
19. U. Schwarz, A. Wosylus, M. Wessel, R. Dronskowski, M. Hanfland, D. Rau, and R. Niewa: High-pressure–high-temperature behavior of Z-Fe_2N and phase transition to $Fe_3N_{1.5}$. *Eur. J. Inorg. Chem.* **2009**, 1634 (2009).
20. W.S. Hummers and R.E. Offeman: Preparation of graphitic oxide. *J. Am. Chem. Soc.* **80**, 1339 (1958).
21. L. Qu, Y. Liu, J.B. Baek, and L. Dai: Nitrogen-doped graphene as efficient metal-free electrocatalyst for oxygen reduction in fuel cells. *ACS Nano* **4**, 1321 (2010).
22. Z.H. Sheng, L. Shao, J.J. Chen, W.J. Bao, F.B. Wang, and X.H. Xia: Catalyst-free synthesis of nitrogen-doped graphene via thermal annealing graphite oxide with melamine and its excellent electrocatalysis. *ACS Nano* **5**, 4350 (2011).
23. Z.H. Wen, X. Wang, S. Mao, Z. Bo, H. Kim, S. Cui, G. Lu, X.L. Feng, and J.H. Chen: Crumpled nitrogen-doped graphene nanosheets with ultrahigh pore volume for high-performance supercapacitor. *Adv. Mater.* **24**, 5610 (2012).
24. Z. Lin, G. Waller, Y. Liu, M.L. Liu, and C.P. Wong: Facile synthesis of nitrogen-doped graphene via pyrolysis of graphene oxide and urea, and its electrocatalytic activity toward the oxygen-reduction reaction. *Adv. Energy Mater.* **2**, 884 (2012).
25. Z. Zhang, B. Lu, J. Hao, W. Yang, and J. Tang: FeP nanoparticles grown on graphene sheets as highly active non-precious-metal electrocatalysts for hydrogen evolution reaction. *Chem. Commun.* **50**, 11554 (2014).
26. J.F. Xie, S. Li, X.D. Zhang, J.J. Zhang, R.X. Wang, H. Zhang, B.C. Pan, and Y. Xie: Atomically-thin molybdenum nitride nanosheets with exposed active surface sites for efficient hydrogen evolution. *Chem. Sci.* **5**, 4615 (2014).
27. P. Xiao, M.A. Sk, L. Thia, X.M. Ge, R.J. Lim, J.Y. Wang, K.H. Lim, and X. Wang: Molybdenum phosphide as an efficient electrocatalyst for the hydrogen evolution reaction. *Energy Environ. Sci.* **7**, 2624 (2014).
28. D. Voiry, H. Yamaguchi, J. Li, R. Silva, D.C. Alves, T. Fujita, M. Chen, T. Asefa, V.B. Shenoy, G. Eda, and M. Chhowalla: Enhanced catalytic activity in strained chemically exfoliated WS_2 nanosheets for hydrogen evolution. *Nat. Mater.* **12**, 850 (2013).
29. J. Bockris and E.C. Potter: The mechanism of the cathodic hydrogen evolution reaction. *J. Electrochem. Soc.* **99**, 169 (1952).
30. M. Jafarian, O. Azizi, F. Gobal, and M.G. Mahjani: Kinetics and electrocatalytic behavior of nanocrystalline conife alloy in hydrogen evolution reaction. *Int. J. Hydrogen Energy* **32**, 1686 (2007).
31. J.L. Shi, Z.H. Pu, Q. Liu, A.M. Asiri, J. Hu, and X.P. Sun: Tungsten nitride nanorods array grown on carbon cloth as an efficient hydrogen evolution cathode at all pH values. *Electrochim. Acta* **154**, 345 (2015).
32. B.E. Conway, V. Birss, and J. Wojtowicz: The role and utilization of pseudocapacitance for energy storage by supercapacitors. *J. Power Sources* **66**, 1 (1997).
33. J. Kubisztal, A. Budniok, and A. Lasia: Study of the hydrogen evolution reaction on nickel-based composite coatings containing molybdenum powder. *Int. J. Hydrogen Energy* **32**, 1211 (2007).
34. L. Liao, S. Wang, J. Xiao, X. Bian, Y. Zhang, M.D. Scanlon, X.L. Hu, Y. Tang, B.H. Liu, and H.H. Girault: A nanoporous molybdenum carbide nanowire as an electrocatalyst for hydrogen evolution reaction. *Energy Environ. Sci.* **7**, 387 (2014).

https://doi.org/10.1557/jmr.2017.138 Published online by Cambridge University Press